The Journal of Phytopharmacology 2023; 12(6):341-357
Online at: www.phytopharmajournal.com

Research Article

ISSN 2320-480X
JPHYTO 2023; 12(6): 341-357
November- December
Received: 29-10-2023
Accepted: 22-12-2023

doi: 10.31254/phyto.2023.12601

Mudassir Alam
Department of Zoology, Aligarh Muslim University, Aligarh, India

Kashif Abbas
Department of Zoology, Aligarh Muslim University, Aligarh, India

Mohd Faizan Saifi
Department of Zoology, Aligarh Muslim University, Aligarh, India

S Mohd. Hasan Abedi
Department of Zoology, Aligarh Muslim University, Aligarh, India

Mohsin Hussain
Department of Chemistry, Aligarh Muslim University, Aligarh, India

Sahab Kausar
Department of Statistics and Operations Research, Aligarh Muslim University, Aligarh, India

Correspondence:
Dr. Mudassir Alam
Department of Zoology, Aligarh Muslim University, Aligarh, India
Email: gh7949@myamu.ac.in

Rosehip Phytochemicals: A Computational Approach for Inhibiting Protein Kinase C Delta in Hepatocellular Carcinoma Treatment

Mudassir Alam, Kashif Abbas, Mohd Faizan Saifi, S Mohd. Hasan Abedi, Mohsin Hussain, Sahab Kausar

ABSTRACT

Hepatocellular carcinoma is a primary liver cancer that is responsible for a significant number of cancer-related deaths worldwide. The development and progression of hepatocellular carcinoma is a complex process that involves various signalling pathways and molecular mechanisms. One such pathway is the protein kinase C delta pathway, which has been shown to play a critical role in the development and progression of hepatocellular carcinoma. Diagnosis of hepatocellular carcinoma employs different techniques including use of imaging tools and biomarkers such as alpha-fetoprotein, des-gamma-carboxyprothrombin, Glypican-3, and protein kinase C delta. protein kinase C delta is a member of the protein kinase C family of serine/threonine kinases that regulates various cellular processes, including cell proliferation and differentiation. Inhibition of protein kinase C delta has been proposed as a potential therapeutic strategy for hepatocellular carcinoma. Several protein kinase C delta inhibitors have been developed and tested in preclinical studies, and some have shown promising results in inhibiting hepatocellular carcinoma cell proliferation and inducing apoptosis. Rosehip of various *Rosa* species are rich in biologically active compound which possess therapeutic properties such as anti-inflammatory, anti-cancerous and hepato-protectant. This study employs various bioinformatic tools to assess molecular, biological, and pharmacological activity of phytochemicals present in rosehip against protein kinase C delta. In order to choose hit compounds, a number of factors are taken into account, including biological activity, binding affinity (docking score), pharmacokinetics, physiochemical characteristics, physicochemical properties, ADME/t properties, and biological activity. Six compounds (quercetin, luteolin, p-coumaric acid, gallic acid, ferulic acid, and caffeine) out of 14 docked compounds matched the requirements. These six phytochemicals might be studied in vitro and in vivo to determine their effectiveness and efficiency.

Keywords: Hepatocellular carcinoma, PKC delta, Rosa, Kinases, *In silico.*

INTRODUCTION

Hepatocellular carcinoma (HCC) is one of the most common primary liver cancers, is a significant global health concern with rising incidence rates and poor overall prognosis. It accounts for a significant proportion of cancer-related deaths worldwide, particularly in regions where chronic liver diseases such as viral hepatitis, alcohol abuse, and non-alcoholic fatty liver disease are prevalent. HCC is primarily caused by chronic liver diseases, with the most common risk factors being chronic hepatitis B and C infection [1], liver cirrhosis (often resulting from various causes), alcohol-related liver disease, non-alcoholic fatty liver disease (NAFLD) and non-alcoholic steatohepatitis (NASH), aflatoxin exposure, metabolic disorders, obesity, and diabetes. These factors contribute to genetic and epigenetic alterations in liver cells over time, leading to the development of HCC [2]. However, the diagnosis of HCC is based on the combination of these indicators, imaging examinations, and clinical evaluation, all of which should be performed by trained healthcare experts. Despite advancements in diagnostic and therapeutic approaches, the prognosis for HCC remains unsatisfactory, emphasizing the urgent need for a deeper understanding of the underlying molecular mechanisms driving HCC progression. PKCδ, also known as protein kinase C delta, is a member of the protein kinase C (PKC) family of serine/threonine kinases has emerged out to novel biomarker and therapeutic target for HCC. It is an enzyme that plays a crucial role in various cellular processes, including cell proliferation, survival, apoptosis, differentiation, migration, and gene expression [3]. PKCδ is a part of the more prominent PKC family, which consists of several isoforms (alpha, beta, gamma, delta, epsilon, eta, theta, iota, lambda, and zeta), each with distinct cellular functions and regulatory properties [4]. PKC isoforms are involved in intracellular signalling pathways and are activated in response to various extracellular stimuli, including growth factors, hormones, and cellular stress. PKCδ is primarily located in the cytoplasm but can translocate to different

cellular compartments, such as the plasma membrane, nucleus, and mitochondria, upon activation [5]. Its translocation is typically triggered by binding to second messengers, such as diacylglycerol (DAG) and calcium ions (Ca2+), which activate PKC signalling [6]. Once activated, PKCδ phosphorylates target proteins, leading to the modulation of downstream signalling pathways. These pathways can regulate diverse cellular processes, including cell proliferation, survival, apoptosis, cytoskeletal dynamics, migration, and angiogenesis. The dysregulation of PKCδ signalling has been implicated in various diseases, including HCC. It plays a significant role in hepatocellular carcinoma (HCC). It promotes cell proliferation, survival, migration, invasion, and angiogenesis in HCC. PKCδ enhances HCC cell growth, suppresses apoptosis, and facilitates the spread of cancer cells. It also contributes to the development of blood vessels to support tumour growth. Furthermore, it interacts with signalling pathways like PI3K/Akt, MAPK/ERK, and Wnt/β-catenin, influencing HCC progression. Targeting PKCδ could be a potential therapeutic approach for HCC [7]. Rosehip phytochemicals have shown promising potential as anti-inflammatory, anti-cancerous and hepatoprotective agents [8]. Rosehips are the fruits of the wild rose plant (*Rosa* spp.) and are rich in various bioactive compounds, including phenolic acid, flavonoids, and carotenoids (Table 1) [9]. This study employs various bioinformatic tools to chalk out the molecular, biological, and pharmacological properties of the phytochemicals present in rosehip in the context of PKCδ.

DIAGNOSIS AND BIOMARKERS FOR HCC

HCC is often diagnosed using a combination of procedures. These include a comprehensive review of the patient's medical history, a physical examination, different blood tests, imaging examinations, and, in some cases, a biopsy. Among the most often used diagnostic markers for HCC are alpha-fetoprotein (AFP), which is typically high in HCC but is not unique to it, and des-gamma-carboxyprothrombin (DCP), which may be especially beneficial when AFP levels are not elevated[10]. Glypican-3 (GPC3) is another marker that may help in the diagnosis of HCC. Furthermore, carcinoembryonic antigen (CEA) is a tumour marker that may be raised in HCC, although it is not unique to this kind of cancer. Human hepatocyte growth factor (HGF) and specific microRNAs such as miR-21, miR-122, and miR-224 are also being studied for their potential diagnostic utility in HCC [11].

3. MATERIAL AND METHODS

Prediction and validation of target protein

PKCδ sequence retrieved from Uniprot database[12] (ID: Q05655) was used as protein query sequences for modelling. SWISS-MODEL (http:// swissmodel.expasy.org) [13] was used for homology modelling to evaluate 3D structure of PKCδ. Different methods were utilised to analyse the inner homogeneity and stability of the PKCδ-modelled structure. The PROCHECK [14] and MolProbity[15] programmes were used to assess the stereochemical quality of projected model with residues of protein in favoured zone of Ramachandran plot. Using GMQE (Global Model Quality Estimate), Ramachandran plot, MolProbity score (http://swissmodel.expasy.org/docs/structure assessment), protein assembly was re-checked for its quality and reliability.

Ligand retrieval and preparation

Structure of phytochemicals present in rosehip were obtained in sdf file format from Pub-Chem database. The Pub-Chem database provides information on organic compounds, such as their molecular structure, formula, and molecular weight (MW) (https://pubchem.ncbi.nlm.nih.gov/source/15751). Table 2 contains information on the compound. OpenBabel[16] tool from PyRx 0.8[17] was used for ligand preparation. Ligand energy was minimised using mmff94 force field. SDF file format of the ligands was converted to pdbqt format to make it executable.

Molecular Docking

A molecular docking research was performed utilising rosehip compounds as ligand group and PKCδ as a macromolecule. The AutoDock Vina [18] tool from PyRx 0.8 was utilised to conduct the molecular docking investigation.

Visualization of Docking Result and interaction

Following the docking simulation, the docked position of ligand with best negative score (docking score) was chosen as hit ligand for target. To explore bound interactions, Discovery Studio 4.5[19] was employed visualise and display the best-docked position.

Estimation of Physiochemical Properties

DruLito programme [20] was incorporated to evaluate the compounds' drug-like characteristics. This study established the amount of rotatable bonds and breaches of Lipinski's rule of 5[21] that orally active medicines must have to show their pharmacological integrity.

Prediction of physicochemical properties

SwissADME [22] server (http://www.swissadme.ch/) was used to foresee and analyse physicochemical features of compounds present in rosehip.

Prediction of absorption, metabolism and distribution

Absorption, distribution, and metabolism prediction of the chosen compound were done using admetSAR[23] (http://lmmd.ecust.edu.cn/admetsar2/).

Prediction of toxicity

ProTox-II [24] (https://tox-new.charite.de/protox_II/index.php?site=compound_input) has been used for toxicity prediction of chosen compound. It is a web-based virtual toxicity laboratory for predicting several toxicological endpoints connected to a chemical structure. It is accessible to academic and non-commercial users. ProTox-II includes computer-based models trained on actual data (in vitro or in vivo) to forecast the hazardous potential of current and hypothetical substances.

Prediction of biological activity of the compound

To predict the biological activities of the selected compounds, the PASS web server [25] (http://www.pharmaexpert.ru/passonline) was employed. The PASS analysis, which employs multilayer atom neighbour descriptors, assists in evaluating the effects of a pharmaceutical entirely on the basis of its molecular formula, meaning that its biological behaviour is completely governed by its chemical structure.

RESULT

Structure prediction and validation

The PKCδ was modelled homologically by utilising the SWISS-MODEL simulated protein modelling server, which is driven by ProMod3. This engine is an open structure comparative modelling tool (Figure 1a). The Ramachandran plot was used to assess the PKCδ model, and it was found that all amino acid residues of the protein model were located within the permissible regions of the plot (Figure 1b). Figure 2 shows that PKCδ had a MolProbity score of 1.17, with 92.14% of its residues located in the favoured regions and only 1.63% in the outlier regions. The Clash score was 0.37. A GMQE value of 0.80 was reported for the structure. The GMQE (Global Model Quality Estimate) is a measure of quality that takes into account both the alignment between the objective and the template, as well as the structure of the template (Figure 3). The final model's lDDT score is predicted with the assistance of a multilayer perception. Value of GMQE ranges between 0 and value, with 1 one being high accuracy of modelled structure and vice-versa. The credibility and acceptability of the suggested homology model is supported by the GMQE scores of PKCδ, which was found to be 0.80. The alignment of the query sequence with the template is illustrated in Figure 4. The UCLA SAVES 6.0 server was utilised to assess the stereochemical quality of a protein structure through residue-by-residue geometry and overall structure geometry evaluation using PROCHECK. Figure 5 displays the Ramachandran plot for all residue types, which was computed using PROCHECK.

Docking score of the compounds

3D crystal structure of predicted PKCδ was used for docking study. Autodock Vina from PyRx 0.8 was used for analysis. Protein was converted to macromolecule and all the selected compounds were first minimised with mmff94 forcefield and then finally converted to pdbqt format suing OpenBabel in PyRx. Blind docking was performed with grid box dimension (98.50 Å ×91.50 Å ×72.99 Å) and centre (2.41, 5.03, -0.30). The exhaustiveness was set to 8 by default. Table 3 summarises the details of ligands or compounds with their docking score. Best docked poses and schematic 2D representation of their interaction with target protein is given in Figure 6 (a-n). We observed that all the chosen compound present in rosehip shown good docking score.

Protein-ligand interaction

Different types of interaction such as Van der Waals, pi and hydrogen bonding emphasise protein-ligand interactions. Detailed information regarding interaction between ligand and target group is showcased in Table 4. Alpha carotene demonstrates van der Waals interactions with specific residues, including Gly206, Thr209, and Asn2014, along with pi interactions involving Lys157 and Leu279. Conversely, beta carotene engages in van der Waals interactions with Pro53, Glu54, and Met427, while also participating in pi interactions with Arg144 and Leu355. Caffeic acid establishes van der Waals forces with Lys176 and Thr242, as well as pi interactions with Phe171, and concurrently forms hydrogen bond interactions with Ser240 and other residues. Chlorogenic acid manifests van der Waals interactions with Leu355 and Gly356, pi interactions with Val363 and Ala376, and hydrogen bond interactions, including those with Arg144 and Lys357. Ferulic acid interacts through van der Waals forces with Leu355 and Glu356, engages in pi interactions with Val363 and Ala376, and forms hydrogen bond interactions with Arg144 and Asp477. Gallic acid exhibits van der Waals interactions with residues such as Leu355 and Val363, pi interactions with Leu480, and hydrogen bond interactions involving Arg144 and Asn478. Kaempferol-3-glucoside establishes van der Waals interactions with Tyr374 and Phe429, pi interactions with Leu673, and hydrogen bond interactions with His412 and other relevant residues. Lutein engages in van der Waals interactions with various residues, including Lys157 and Glu206, as well as pi interactions with Ile205 and Arg207. Luteolin exhibits van der Waals interactions with residues Ile205 and Gly206, along with hydrogen bond interactions involving Arg207 and Thr218. p-Coumaric acid interacts through van der Waals forces with Arg144 and Leu355, pi interactions with Val363 and Ala376, and hydrogen bond interactions with Asp477. Quercetin demonstrates van der Waals interactions with residues such as Leu355 and Gly356, pi interactions with Val363 and Ala376, and hydrogen bond interactions with Arg144 and Lys357. Isoquercetin engages in van der Waals interactions with Phe429 and Asp482, pi interactions with Leu673, and hydrogen bond interactions with Tyr374 and His412. Rutin exhibits van der Waals interactions with residues like Met1 and Thr58, pi interactions with Phe4 and Met142, and hydrogen bond interactions with Arg6 and Met51. Finally, zeaxanthin interacts through van der Waals forces with residues Met5 and Tyr52, pi interactions with Arg144 and Leu355, and hydrogen bond interactions with various amino acids.

Pharmacokinetics and Toxicological Properties Analysis

To evaluate drug-likeness of a compound, ADME/t characteristics of ligands must be determined. The pharmacological characteristics of compounds found in rosehip extract were assessed using the DruLito programme. Drug-likeness rules (Lipinski's rule, MDDR-like rule, Ghose filter, BBB similarity, CMC-50-like rule, unweighted QED, Veber filter, and weighted QED) compute and filter may be used to identify compounds. The observations are summarised in the Table 5. Alpha and Beta Carotene exhibit high lipophilicity with substantial logP and AlogP values, coupled with a lack of hydrogen bond acceptors and donors. Caffeic Acid displays moderate lipophilicity, a moderate polar surface area, and a modest number of rotatable bonds. Gallic Acid, in contrast, demonstrates higher polar surface area and moderate lipophilicity. Chlorogenic Acid has a negative logP, indicating hydrophilicity, and showcases a considerable number of hydrogen bond acceptors and donors, reflecting its potential for hydrogen bonding interactions. Ferulic Acid exhibits moderate lipophilicity, a moderate polar surface area, and a moderate number of rotatable bonds. Kaempferol-3-Glucoside is hydrophilic with a substantial polar surface area and multiple rotatable bonds. Lutein and Zeaxanthin are lipophilic with moderate polar surface areas. Luteolin shows moderate lipophilicity, a moderate polar surface area, and a few rotatable bonds. p-Coumaric Acid exhibits moderate lipophilicity, a moderate polar surface area, and a single rotatable bond. Quercetin and Rutin showcase significant hydrogen bonding capacity, contributing to their potential interactions in biological systems. Isoquercetin, highly hydrophilic, boasts an extensive polar surface area and numerous rotatable bonds. Out of 14, compounds, six compounds showed drug-likeness on the basis above mentioned rules and parameters. Physicochemical properties of the compound calculated using SWISSADME server are given in Table 6. Comparative data between the observed values of the compounds and the standard values are visually represented in Figure7. Using the admetSAR server, absorption, distribution, and metabolism of compounds with drug-likeness was predicted as illustrated in Table 7. Table 5, 6 and 7 summarises the result.

Protox II server was used for toxicity prediction of the compounds. Table 8 summarises the result. All the chosen molecules were safe and shown negligible or no sign of any toxicity as per Protox II server.

Predictions of Biological Activity of Compounds

The PASS webserver was used to authorize the predicted biological activity, and the chosen phytochemicals turned out to have the same biological activities. This study showed that the molecules in series 1–6 possess anticarcinogenic, antineoplastic, hepatoprotective properites, and may act as protein kinase c delta inhibitor. Pa ranges from 0.605 to 0.689 for anti-inflammatory, for anticarcinogenic and it goes from 0.395 to 0.757. For antineoplastic activity, Pa values ranges between 0.158 and 0.797. Further, Pa value range for hepatoprotection, kinase inhibitor and protein kinase inhibitor activity are 0.461-0.706, 0.246-0.984, 0.045-0.115 respectively. When Pa > Pi, the above Pa values show that the molecules are likely to have strong biological activity. The prediction is summed up in the table 9.

DISCUSSION

The investigation presented herein focuses on the homology modeling of Protein Kinase C delta (PKCδ) and the subsequent assessment of its structural robustness. Additionally, docking study was conducted, specifically concentrating on interactions with various compounds found in rosehip. The analyzed compounds encompass Alpha and Beta Carotene, Caffeic Acid, Gallic Acid, Chlorogenic Acid, Ferulic Acid, Kaempferol-3-Glucoside, Lutein, Zeaxanthin, Luteolin, p-Coumaric Acid, Quercetin, Rutin, and Isoquercetin. These compounds were evaluated for their lipophilicity, polar surface area, and hydrogen bonding capacity, with a subsequent examination of their biological activities. The homology modeling utilized the SWISS-MODEL server with ProMod3, ensuring the fidelity of the PKCδ model. Validation metrics such as the Ramachandran plot and MolProbity score confirmed structural integrity, with the majority of residues falling within acceptable regions. The GMQE score of 0.80 substantiated the reliability of the homology model, indicating its accuracy compared to the template structure. Autodock Vina facilitated the docking study, revealing satisfactory scores for all selected phytochemicals. The ligand-protein complexes were visualized using DiscoveryStudio to elucidate the binding sites. Notably, Quercetin, Isoquercetin, and Rutin exhibited particularly promising interaction profiles. Quercetin demonstrated diverse interactions, including van der Waals interactions, pi interactions, and hydrogen bond interactions, suggesting a versatile and stable binding pattern. Isoquercetin and Rutin similarly displayed comprehensive binding profiles indicative of strong affinity and stability. The chosen phytochemicals were further assessed for drug-likeness, with Caffeic Acid, Ferulic Acid, Gallic Acid, Luteolin, p-Coumaric Acid, and Quercetin exhibiting favorable properties. Subsequent ADME and toxicity predictions using the Protox II server indicated the safety of these compounds, with negligible or no signs of toxicity. Finally, the biological activities of the six selected compounds were evaluated, revealing anti-inflammatory, anti-carcinogenic, anti-neoplastic, hepatoprotective, kinase inhibitor, and protein kinase inhibitor activities. Previous studies have proposed that phytochemicals present in rosehip possess anti-cancerous and hepatoprotective properties [26, 27]. These findings support the fact that rosehip phytochemicals, particularly the identified compounds, may serve as potent agents in addressing various health concerns, including cancer.

CONCLUSION

Hepatocellular carcinoma (HCC) is the most common type of primary liver cancer, accounting for about 75-85% of cases. In this study, phytochemicals present in rosehip of *Rosa* species are screened against PKCδ for their potency to be its inhibitor. Various parameters such as pharmacokinetics, physiochemical properties, physicochemical properties, ADME/t properties, biological activity, and binding affinity (docking score) are taken into consideration to select hit compounds. Out of 14 docked compounds, 6 compounds (caffeic acid, ferulic acid, gallic acid, p-coumaric acid, luteolin and quercetin) shown to meet the above parameters including good docking score, drug-likeness, safe and having biological activities such as anti-inflammatory, anticarcinogenic, antineoplastic, hepatoprotective, kinase inhibitor and protein kinase inhibitor. These 6 compounds could be further investigated for its efficiency and efficacy using in vitro and in vivo.

Table 1: Phytochemicals present in rosehip of *Rosa* sp

CLASS	COMPOUND NAME
Phenolic acid	Gallic acid Chlorogenic acid Caffeic acid p-coumaric acid Ferulic acid
Flavonoids	Rutin Kaempferol-3-*O*-glucoside Luteolin Quercetin Isoquercetin
Carotenoids	α-carotene β-carotene lutein zeaxanthin

Table 2: Compounds present in rosehip with their molecular weight and PubChem ID

Ligand name	MW (g/mol)	PUBCHEM ID
Alpha carotene	536.9	6419725
Beta carotene	536.9	5280489
Caffeic acid	180.16	689043
Chlorogenic acid	354.31	1794427
Ferulic acid	194.18	445858
Gallic acid	170.12	370
Kaempferol-3-glucoside	448.4	5282102
Lutein	568.9	5281243
Luteolin	286.24	5280445
p-Coumaric acid	164.16	1549106
Quercetin	302.23	5280343
Isoquercetin	464.4	5280804
Rutin	610.5	5280805
Zeaxanthin	568.9	5280899

Table 3: Compounds with their docking score

Ligand	MW (g/mol)	PUBCHEM ID	Docking score (kcal/mol)
Alpha carotene	536.9	6419725	-8.7
Beta carotene	536.9	5280489	-8.0
Caffeic acid	180.16	689043	-8.8
Chlorogenic acid	354.31	1794427	-7.9
Ferulic acid	194.18	445858	-7.2
Gallic acid	170.12	370	-7.7
Kaempferol-3-glucoside	448.4	5282102	-7.8
Lutein	568.9	5281243	-9.1
Luteolin	286.24	5280445	-8.1
p-Coumaric acid	164.16	1549106	-8.9
Quercetin	302.23	5280343	-7.9
Isoquercetin	464.4	5280804	-7.7
Rutin	610.5	5280805	-9.1
Zeaxanthin	568.9	5280899	-8.7

Table 4: Interaction between selected ligand compound and the target protein

Ligand name	Van der waals interaction	pi interaction	Hydrogen bond interaction
Alpha carotene	Gly206, Thr209, Asn2014, Thr218, Glu223, Arg224, Asn226, Ile227, Glu274, Val276, Ala277, Asn278, Thr295	Lys157, Ile205, Arg207, Phe225, Leu279, Leu291	----------
Beta carotene	Pro53, Glu54, Ser57, Thr58, Asn143, Arg145, Gly146, Gly356, Lys357, Met427, Asp434, Lys457, Asp477, Asn478, Asp491, Glu636	Arg144, Leu355, Val365, Ala376, Leu480, Ala490, Phe633, Phe637	----------
Caffeic acid	Lys176, Thr242, Asp245	Phe171	Ser240, Pro241, Phe243, Asn267
Chlorogenic acid	Leu355, Gly356, Gly358, Lys378, Thr411, Met427, Asp434, Asp477, Phe633, Phe637	Val363, Ala376, Leu480, Ala490	Arg144, Lys357, Asp491
Ferulic acid	Leu355, Glu356, Thr411, Glu428, Asp434, Asp491, Phe633, Phe637	Val363, Ala376, Lys378, Met427, Leu480, Ala490	Arg144, Asp477
Gallic acid	Leu355, Val363, Ala376, Phe429, Asp434, Asp477, Ala490, Asp491, Phe633, Asp634	Leu480	Arg144, Asn478
kaempferol-3-glucoside	Tyr374, Phe429, Asp482, Asp484, Val624, Phe670, His672	Leu673	His412, Glu428, Arg483, Lys488, Arg614, Pro627
Lutein	Lys157, Glu206, Thr209, Asn214, Glu223, Phe225, Arg273, Glu274, Asn278, Val294, Thr295	Ile205, Arg207, Arg224, Ile227, Pro230, Ala277, Leu279, Leu291	----------
Luteolin	Ile205, Gly206, Thr209, Asn214, Lys222, Asn226, Ala277, Asn278, Leu279	----------	Arg207, Thr218, Glu221
p-Coumaric acid	Arg144, Leu355, Gly356, Thr411, Met427, Leu430, Asp434, Asn478, Phe633	Val363, Ala376, Leu480, Ala490	Asp477
Quercetin	Leu355, Gly356, Lys378, Thr411, Asp434, Asp477, Asp491, Phe492, Phe633, Phe637	Val363, Ala376, Leu480, Ala490	Arg144, Lys357
Isoquercetin	Phe429, Asp482, Pro627, Phe670, His672	Leu673	Tyr374, His412, Glu428, Asn431, Arg483, Asp484, Lys488, Arg614
Rutin	Met1, Thr58, Phe59, Ala61, Thr141, Asn143, Glu540, Ser548, His549	Phe4, Met142, Arg145, Asp513	Arg6, Met51, Asp60, His62, Asp551
Zeaxanthin	Met5, Tyr52, Pro53, Glu54, Ser57, Thr58, Asn143, Arg145, Gly146, Gly356, Ala376, Lys378, Thr411, Met427, Asp434, Lys475, Asp477, Asn478, Asp491, Glu636	Arg144, Leu355, Val363, Leu480, Ala490, Phe633, Phe637	----------

Table 5: Pharmacological properties of the compounds evaluated using DruLito software

Title	logp	Alogp	HBA	HBD	TPSA	AMR	nRB	nAtom	nAcidicGroup	RC	nRigidB	nAromRing	nHB
Alpha carotene	15.187	9.61	0	0	0	190.91	10	96	0	2	31	0	0
Beta carotene	14.734	8.935	0	0	0	189.29	10	96	0	2	31	0	0
Caffeic acid	0.888	0.203	4	3	77.76	50.41	2	21	1	1	11	1	7
Chlorogenic acid	-0.7	-1.194	9	6	164.75	85.8	5	43	1	2	21	1	15
Ferulic acid	0.78	0.267	4	2	66.76	55.45	3	24	1	1	11	1	6
Gallic acid	0.964	-0.721	5	4	97.99	41.77	1	18	1	1	11	1	9
Kaempferol-3-glucoside	-0.249	-2.771	11	7	186.37	114.53	4	52	0	4	31	2	18
Lutein	11.283	8.621	2	2	40.46	195.47	10	98	0	2	33	0	4
Luteolin	1.486	-0.787	6	4	107.22	81.76	1	31	0	3	22	2	10
p- coumaric acid	0.751	0.766	3	2	57.53	48.8	2	20	1	1	10	1	5
Quercetin	1.834	-1.244	7	5	127.45	83.44	1	32	0	3	23	2	12
Isoquercetin	0.099	-3.334	12	8	206.6	116.14	4	53	0	4	32	2	20
Rutin	-0.735	-4.581	16	10	265.52	147.17	6	73	0	5	41	2	26
Zeaxanthin	10.564	8.49	2	2	40.46	195.39	10	98	0	2	33	0	4

Table 6: Physico-chemical properties of compound as predicted by SWISSADME

Ligand Name	LogS	XLogp3	Solubility	GI absorption	Bioavailability	Lipinski's rule violation	Drug-likeness
Alpha carotene	-11.11	13.65	Insoluble	Low	0.17	YES	NO
Beta carotene	-11.04	13.54	Insoluble	Low	0.17	YES	NO
Caffeic acid	-1.89	1.15	Very soluble	High	0.56	NO	YES
Chlorogenic acid	-1.62	-0.42	Very soluble	Low	0.11	YES	NO
Ferulic acid	-2.11	1.51	Soluble	High	0.85	NO	YES
Gallic acid	-1.64	0.70	Very soluble	High	0.56	NO	YES
Kaempferol-3-glucoside	-3.8	0.72	Soluble	Low	0.17	YES	NO
Lutein	-9.64	11.01	Insoluble	Low	0.17	YES	NO
Luteolin	-3.71	2.53	Soluble	High	0.55	NO	YES
p- coumaric acid	-2.02	1.46	Soluble	High	0.85	NO	YES
Quercetin	-3.16	1.54	Soluble	High	0.55	NO	YES
Isoquercetin	-3.04	0.36	Soluble	Low	0.17	YES	NO
Rutin	-3.30	-0.33	Soluble	Low	0.17	YES	NO
Zeaxanthin	-9.58	10.91	Poorly soluble	Low	0.17	YES	NO

Table 7: admetSAR online toolkit information on the drug-likeness of compounds, including their absorption, distribution, and metabolism

Parameters	Caffeic acid	Ferulic acid	Gallic acid	Luteolin	p-coumaric Acid	Quercetin
ABSORPTION						
BB-barrier	-	-	-	-	-	-
Human intestinal absorption	+	+	+	+	+	+
P-glycoprotein substrate	-	-	-	-	-	-
P-glycoprotein inhibitor						
DISTRIBUTION						
Subcellular localization	-	-	-	-	-	-
METABOLISM	Mitochondria	Mitochondria	Mitochondria	Mitochondria	Mitochondria	Mitochondria
CYP2C9 substrate	Non-substrate	Non-substrate	Non-substrate	Non-substrate	Non-substrate	Non-substrate
CYP2D6 substrate	Non-substrate	Non-substrate	Non-substrate	Non-substrate	Non-substrate	Non-substrate
CYP3A4 substrate	Non-substrate	Non-substrate	Non-substrate	Non-substrate	Non-substrate	Substrate
CYP1A2 inhibition	Non-inhibitor	Non-inhibitor	Non-inhibitor	Inhibitor	Non-inhibitor	Inhibitor
CYP2C9 inhibition	Non-inhibitor	Non-inhibitor	Non-inhibitor	Non-inhibitor	Non-inhibitor	Non-inhibitor
CYP2D6 inhibition	Non-inhibitor	Non-inhibitor	Non-inhibitor	Non-inhibitor	Non-inhibitor	Non-inhibitor
CYP2C19 inhibition	Non-inhibitor	Non-inhibitor	Non-inhibitor	Non-inhibitor	Non-inhibitor	Non-inhibitor

Table 8: Toxicological prediction of the compounds using PROTOX- II server.

Parameters	Caffeic acid	Ferulic acid	Gallic acid	Luteolin	p-coumaric acid	Quercetin
Carcinogenicity	Weak/low	Inactive	Inactive	Inactive	Inactive	Low
Mutagenicity	Inactive	Inactive	Inactive	Inactive	Inactive	Low
Cytotoxicity	Inactive	Inactive	Inactive	Inactive	Inactive	Inactive
Immunotoxicity	Inactive	Low	Inactive	Inactive	Inactive	Inactive
Hepatotoxicity	Inactive	Inactive	Inactive	Inactive	Inactive	Inactive

Table 9: Prediction of the biological activity of compounds (Pa = probability of activity; Pi = probability of inactivity).

Compound name	Biological activity	Pa	Pi
CAFFEIC ACID	Anti-inflammatory	0.651	0.023
	Anticarcinogenic	0.571	0.014
	Antineoplastic	0.190	0.097
	Hepatoprotective	0.461	0.024
	Kinase inhibitor	0.264	0.194
	Protein kinase inhibitor	0.082	0.073
FERULIC ACID	Anti-inflammatory	0.604	0.031
	Anticarcinogenic	0.616	0.012
	Antineoplastic	0.241	0.048
	Hepatoprotective	0.621	0.011
	Kinase inhibitor	0.283	0.165
	Protein kinase inhibitor	0.115	0.104
GALLIC ACID	Anti-inflammatory	0.548	0.044
	Anticarcinogenic	0.395	0.031
	Antineoplastic	0.158	0.144
	Hepatoprotective	0.504	0.020
	Kinase inhibitor	0.388	0.072
	Protein kinase inhibitor	0.102	0.012
LUTEOLIN	Anti-inflammatory	0.661	0.021

	Anticarcinogenic	0.690	0.009
	Antineoplastic	0.783	0.014
	Hepatoprotective	0.658	0.009
	Kinase inhibitor	0.904	0.002
	Protein kinase inhibitor	0.045	0.029
P-COUMARIC ACID	Anti-inflammatory	0.641	0.024
	Anticarcinogenic	0.559	0.015
	Antineoplastic	0.174	0.121
	Hepatoprotective	0.553	0.016
	Kinase inhibitor	0.246	0.225
	Protein kinase inhibitor	----	----
QUERCETIN	Anti-inflammatory	0.689	0.017
	Anticarcinogenic	0.757	0.007
	Antineoplastic	0.797	0.012
	Hepatoprotective	0.706	0.007
	Kinase inhibitor	0.809	0.005
	Protein kinase inhibitor	0.072	0.019

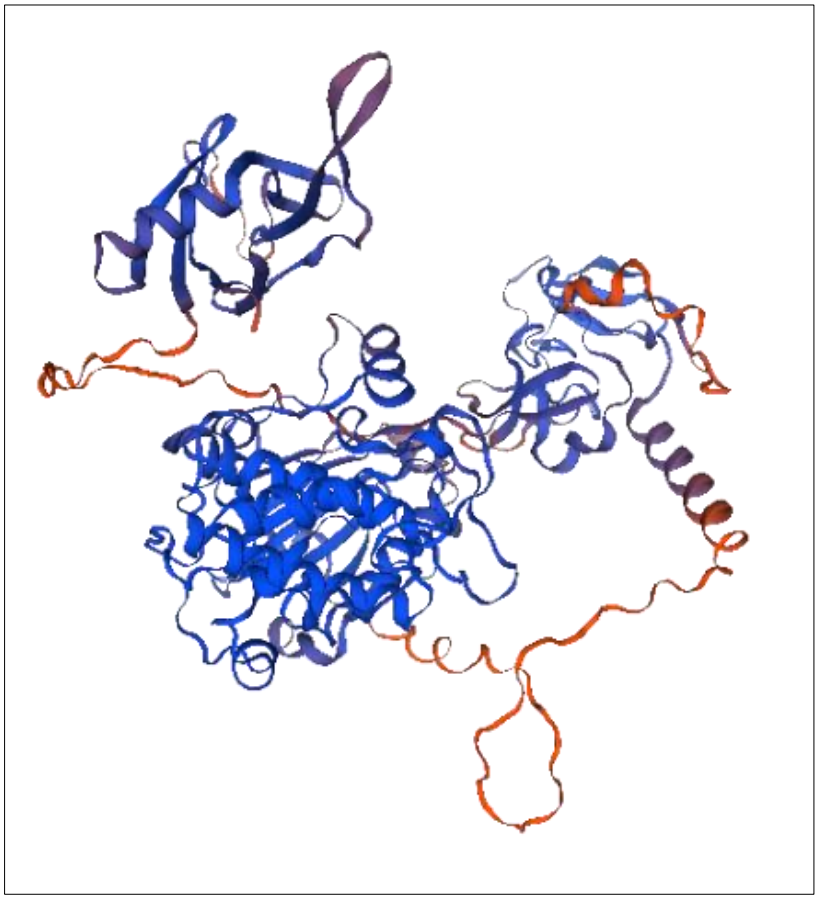

Figure 1 (a): Predicted structure of PKCδ using S SWISS-MODEL.

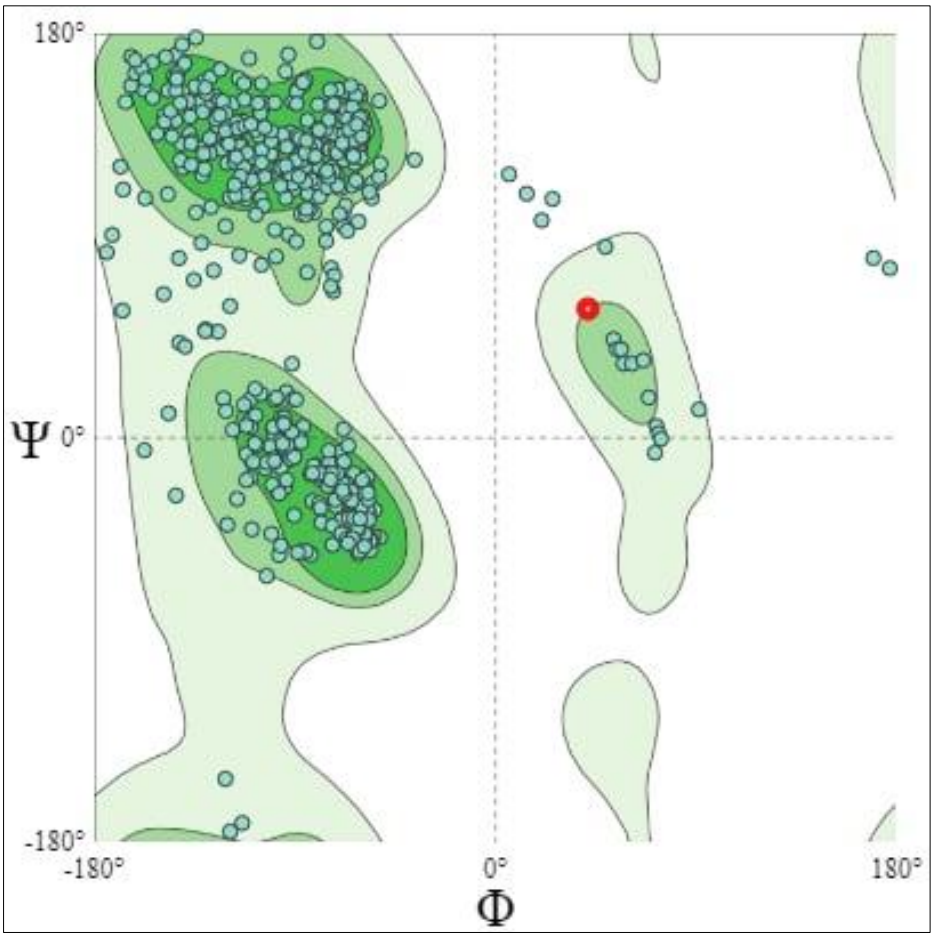

Figure 1 (b): Ramachandran plot for predicted PKCδ structure.

MolProbity Results

MolProbity Score	1.17	
Clash Score	0.37	
Ramachandran Favoured	92.14%	
Ramachandran Outliers	1.63%	A140 PRO, A183 ASN, A313 TYR, A491 ASP, A324 GLY, A129 GLN, A126 ASP, A326 ASP, A341 SER, A320 THR, A132 ARG
Rotamer Outliers	1.18%	A316 PHE, A392 GLU, A202 ASP, A299 SER, A117 SER, A36 LEU, A333 THR
C-Beta Deviations	6	A491 ASP, A130 SER, A136 GLU, A389 ASP, A176 LYS, A183 ASN
Bad Bonds	0 / 5575	

Figure 2: MolProbity report for the predicted structure

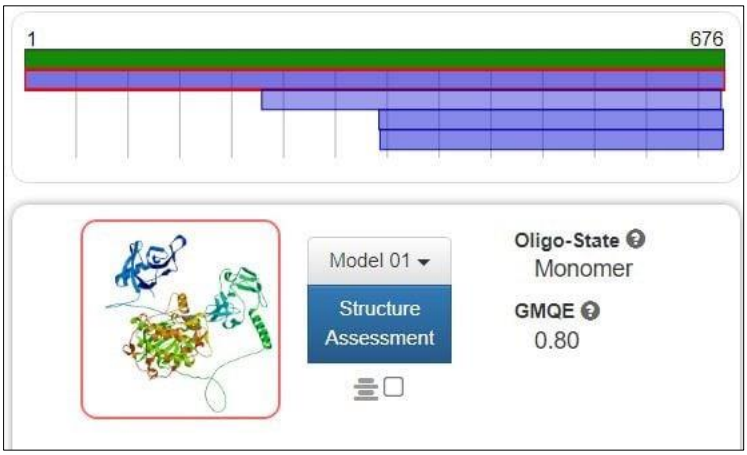

Figure 3: GMQE score for predicted structure of PKCδ

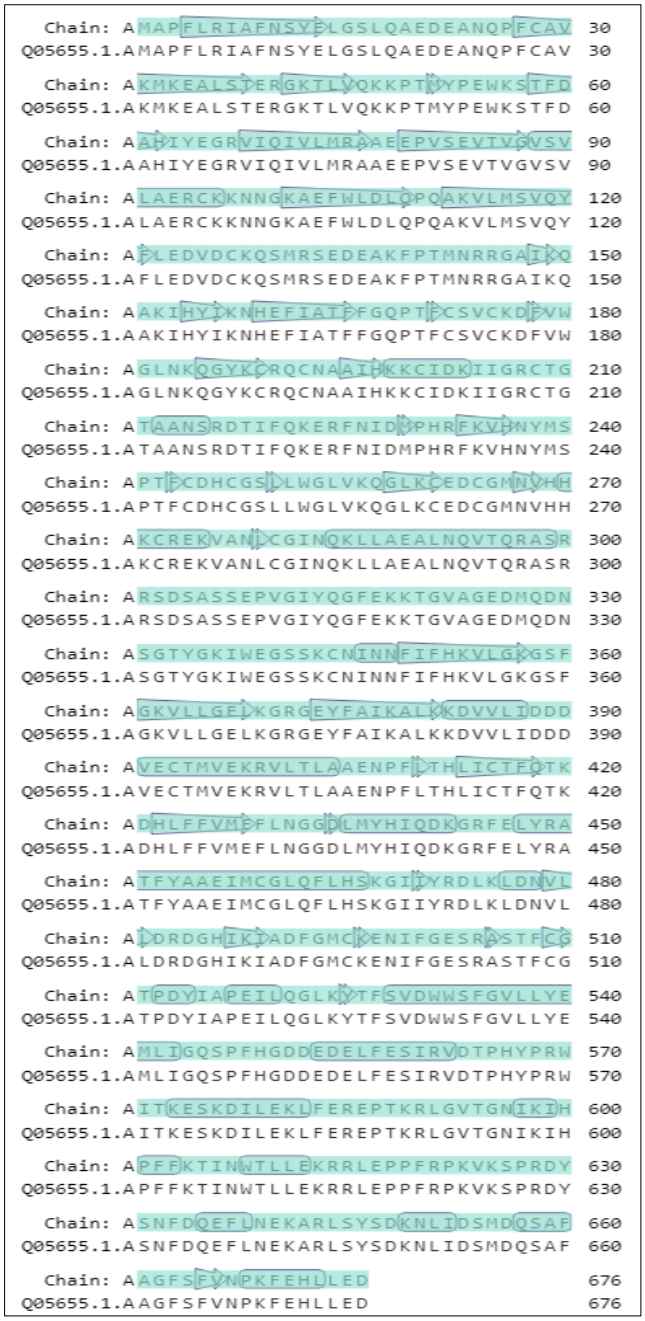

Figure 4: Sequence alignment of query sequence with template

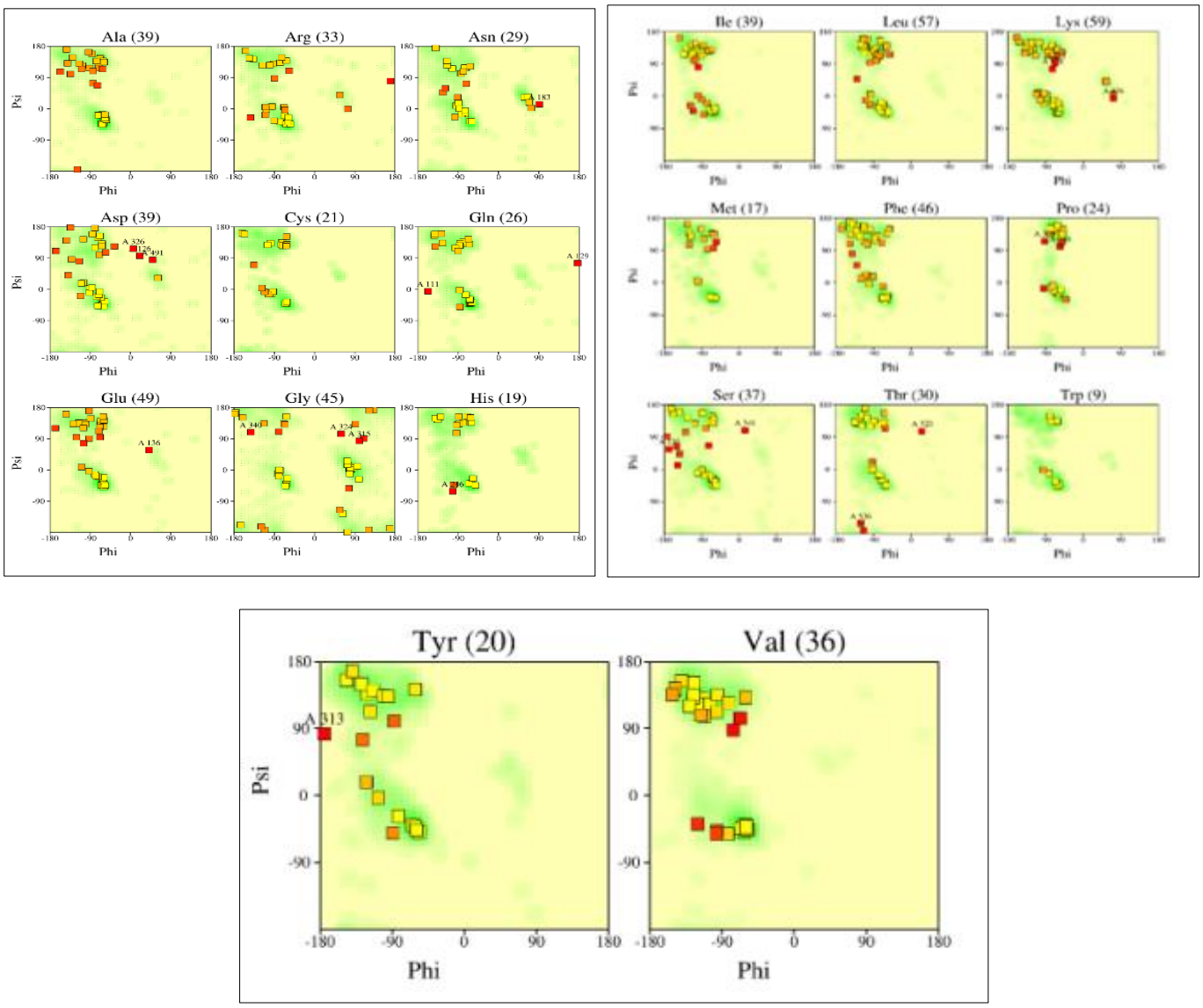

Figure 5: Ramachandran plot for all residue types: The number of residues is shown in parentheses. Those with poor conformations (scoring -3.00) are indicated. According to study of 163 structures at resolution 2.0A or higher, shading reveals advantageous conformations.

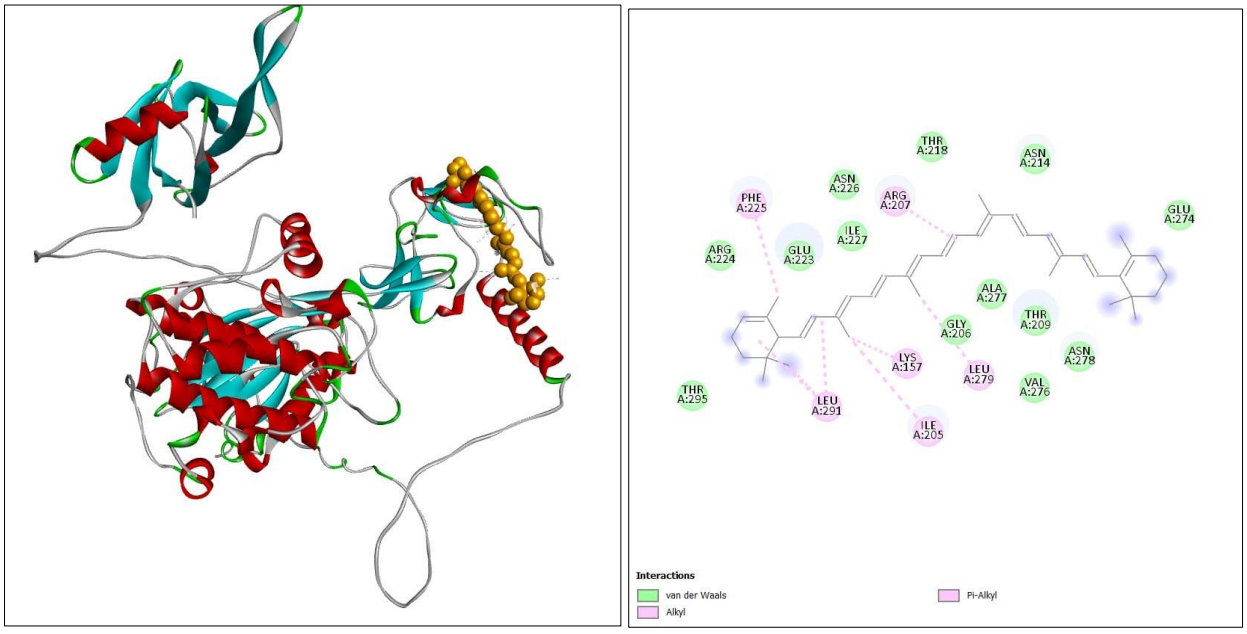

(A)

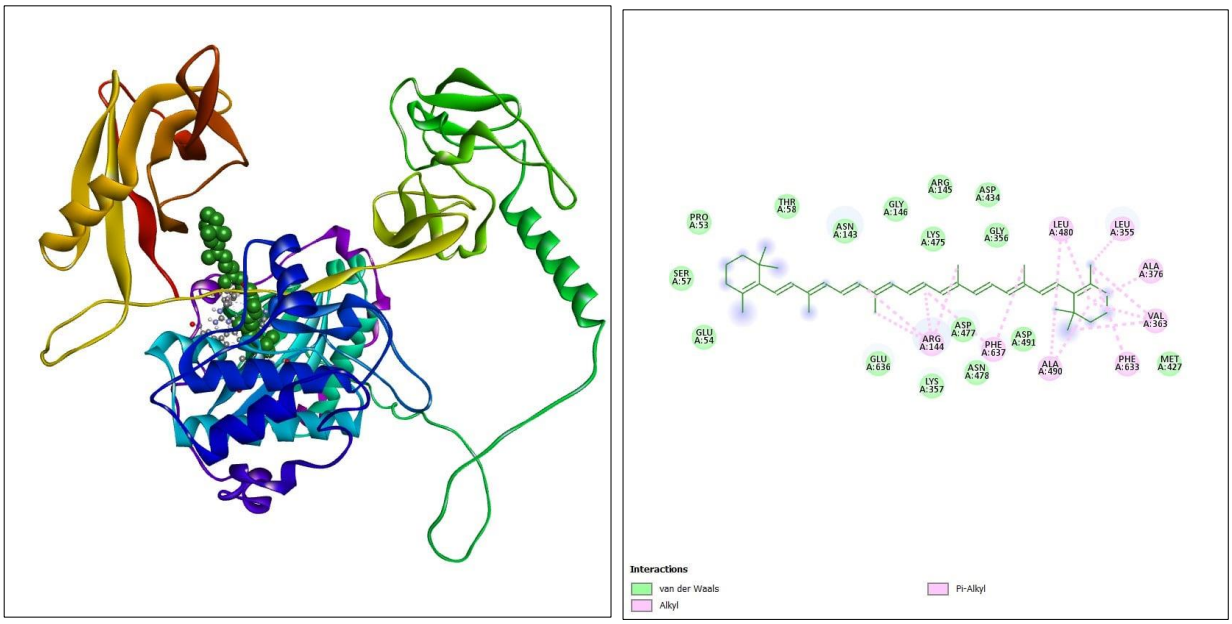
PRO A:53
THR A:58
GLY A:146
ARG A:145
ASP A:434
ASN A:143
LYS A:475
GLY A:356
LEU A:480
LEU A:355
SER A:57
ALA A:376
VAL A:363
GLU A:54
ARG A:144
ASP A:477
PHE A:637
ASP A:491
GLU A:636
ASN A:478
ALA A:490
PHE A:633
MET A:427
LYS A:357
Interactions
van der Waals
Alkyl
Pi-Alkyl

(B)

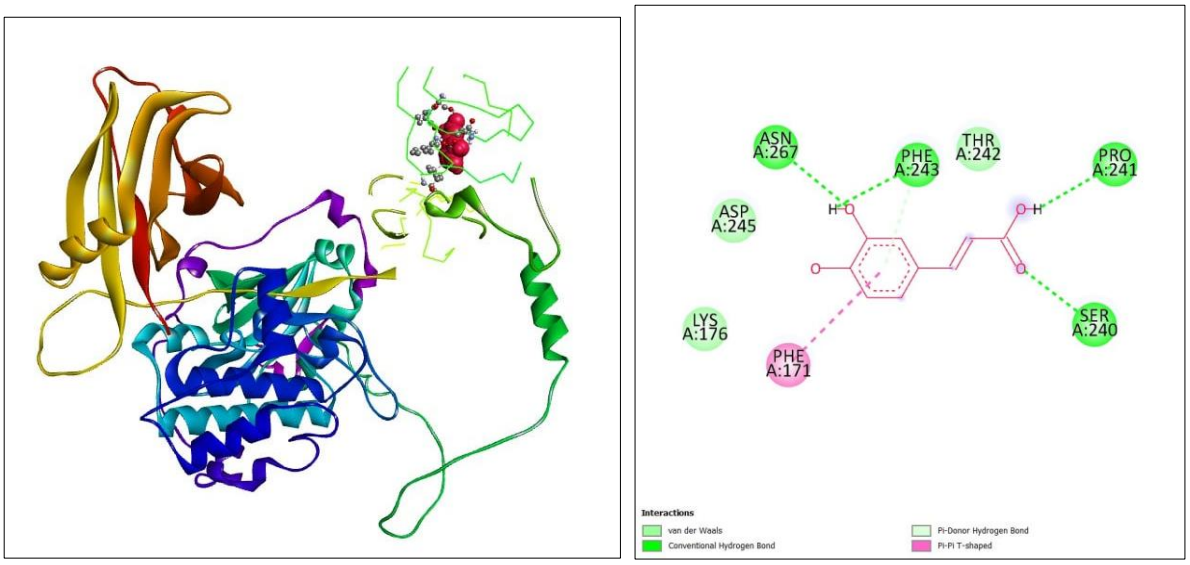
ASN A:267
PHE A:243
THR A:242
PRO A:241
ASP A:245
LYS A:176
PHE A:171
SER A:240
Interactions
van der Waals
Conventional Hydrogen Bond
Pi-Donor Hydrogen Bond
Pi-Pi T-shaped

(C)

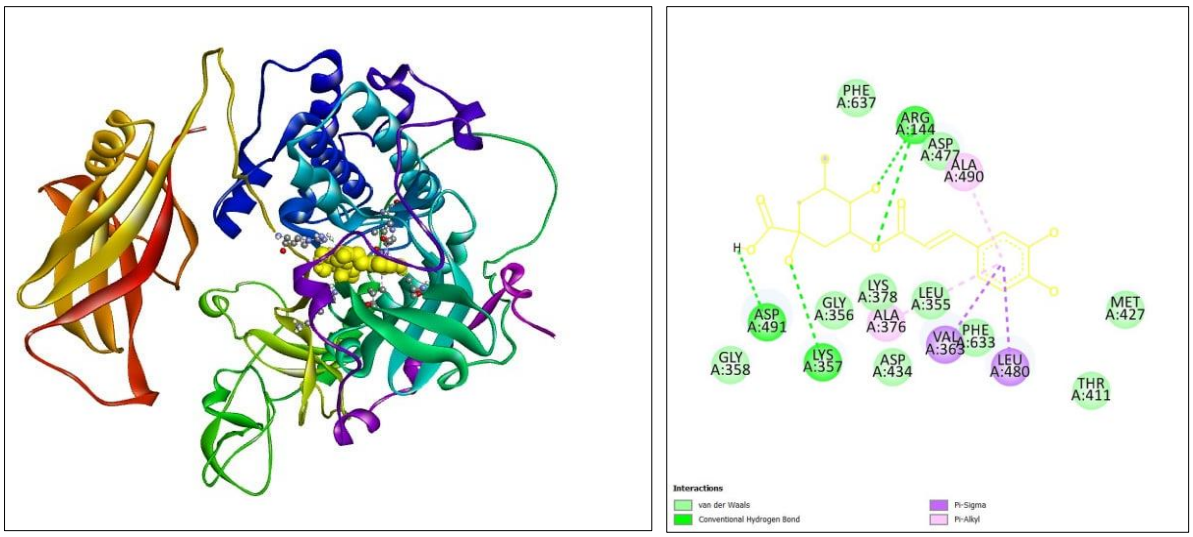
PHE A:637
ARG A:144
ASP A:477
ALA A:490
ASP A:491
GLY A:356
LYS A:378
LEU A:355
ALA A:376
MET A:427
VAL A:363
PHE A:633
GLY A:358
LYS A:357
ASP A:434
LEU A:480
THR A:411
Interactions
van der Waals
Conventional Hydrogen Bond
Pi-Sigma
Pi-Alkyl

(D)

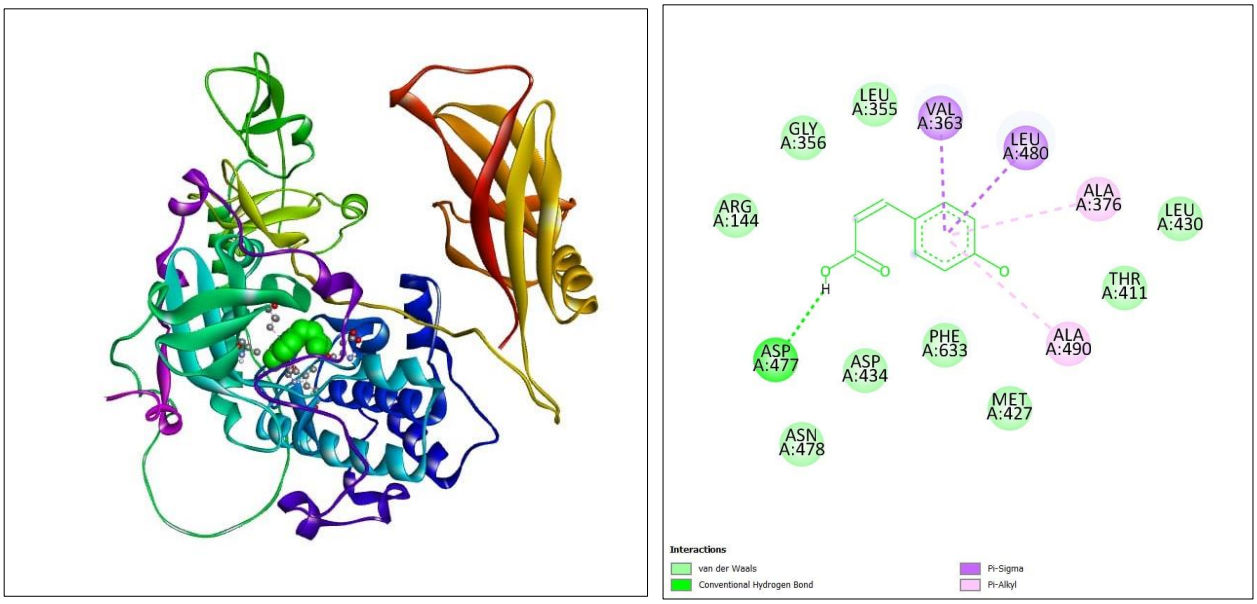
LEU A:355
VAL A:363
GLY A:356
LEU A:480
ALA A:376
ARG A:144
LEU A:430
THR A:411
ASP A:477
PHE A:633
ALA A:490
ASP A:434
MET A:427
ASN A:478
Interactions
van der Waals
Conventional Hydrogen Bond
Pi-Sigma
Pi-Alkyl

(E)

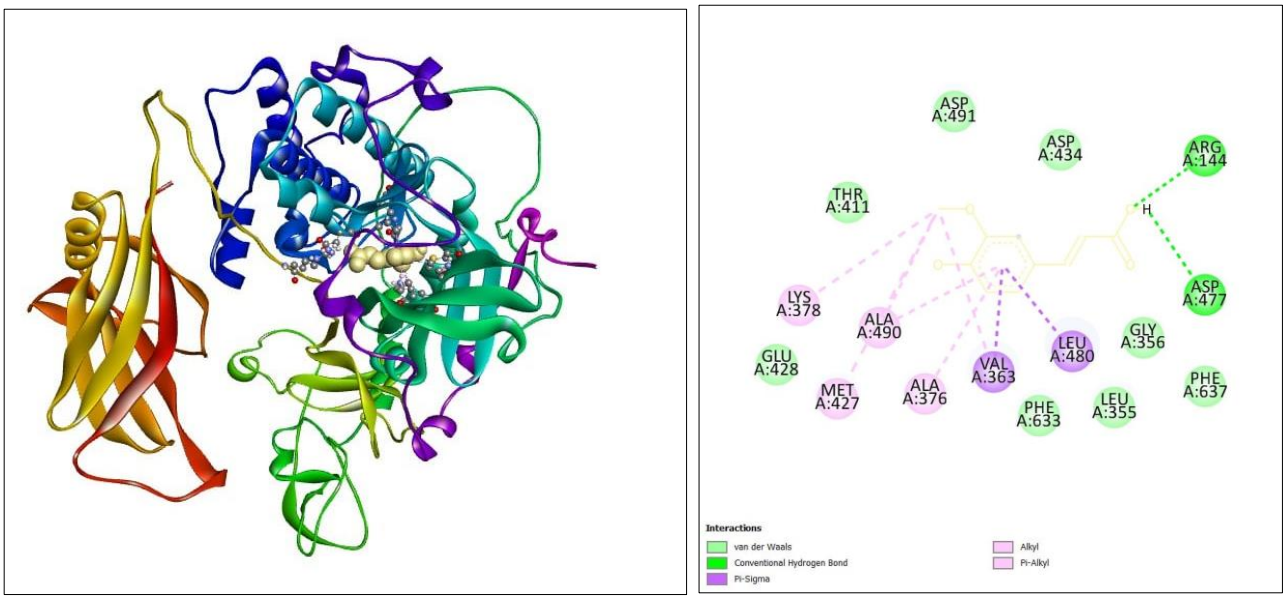
ASP A:491
ASP A:434
ARG A:144
THR A:411
ASP A:477
LYS A:378
ALA A:490
GLY A:356
LEU A:480
GLU A:428
VAL A:363
PHE A:637
MET A:427
ALA A:376
PHE A:633
LEU A:355
Interactions
van der Waals
Conventional Hydrogen Bond
Pi-Sigma
Alkyl
Pi-Alkyl

(F)

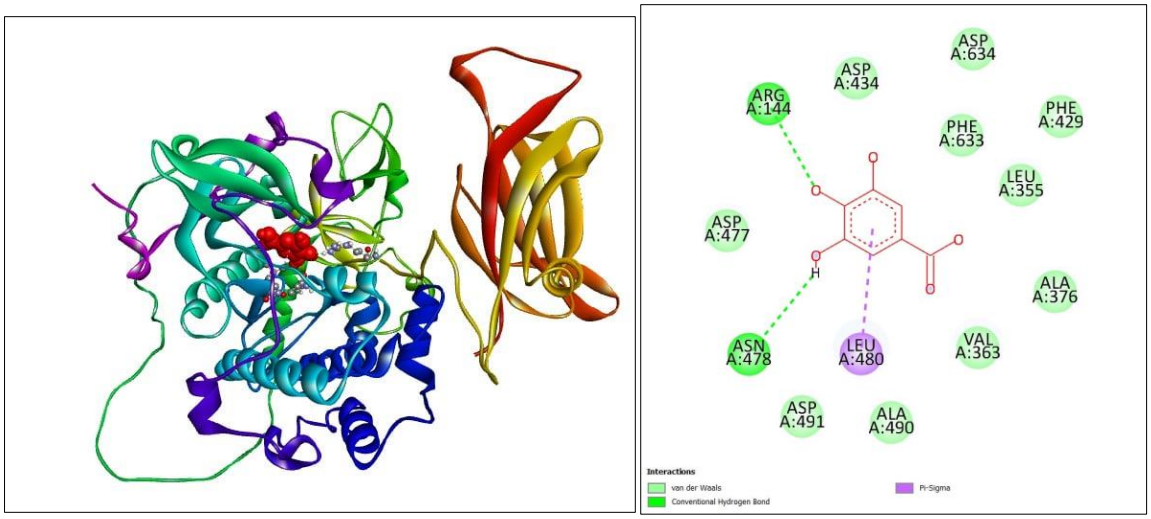
ASP A:634
ASP A:434
ARG A:144
PHE A:429
PHE A:633
LEU A:355
ASP A:477
ALA A:376
ASN A:478
LEU A:480
VAL A:363
ASP A:491
ALA A:490
Interactions
van der Waals
Conventional Hydrogen Bond
Pi-Sigma

(G)

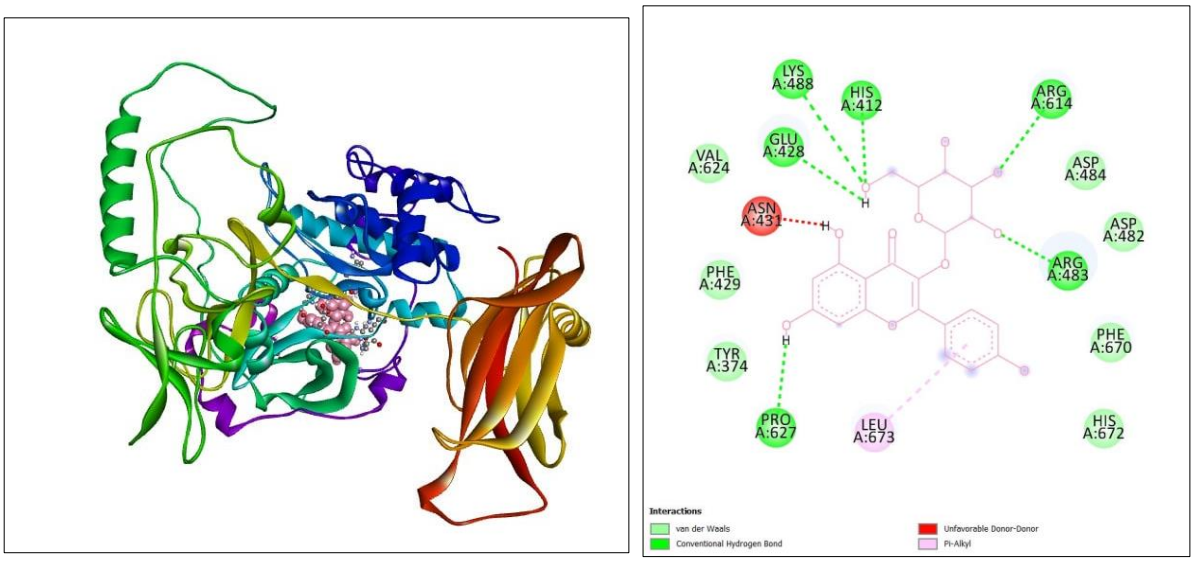
LYS A:488
HIS A:412
ARG A:614
GLU A:428
VAL A:624
ASP A:484
ASN A:431
ASP A:482
ARG A:483
PHE A:429
PHE A:670
TYR A:374
PRO A:627
LEU A:673
HIS A:672
Interactions
van der Waals
Conventional Hydrogen Bond
Unfavorable Donor-Donor
Pi-Alkyl

(H)

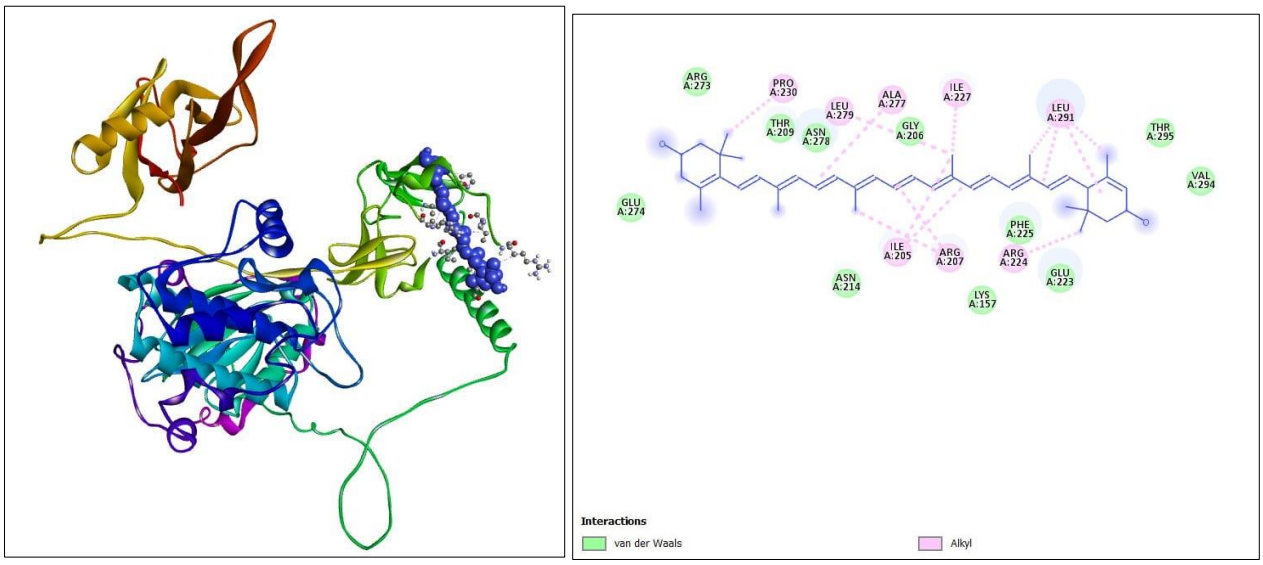
ARG A:273
PRO A:230
LEU A:279
ALA A:277
ILE A:227
LEU A:291
THR A:209
ASN A:278
GLY A:206
THR A:295
VAL A:294
GLU A:274
PHE A:225
ILE A:205
ARG A:207
ARG A:224
GLU A:223
ASN A:214
LYS A:157
Interactions
van der Waals
Alkyl

(I)

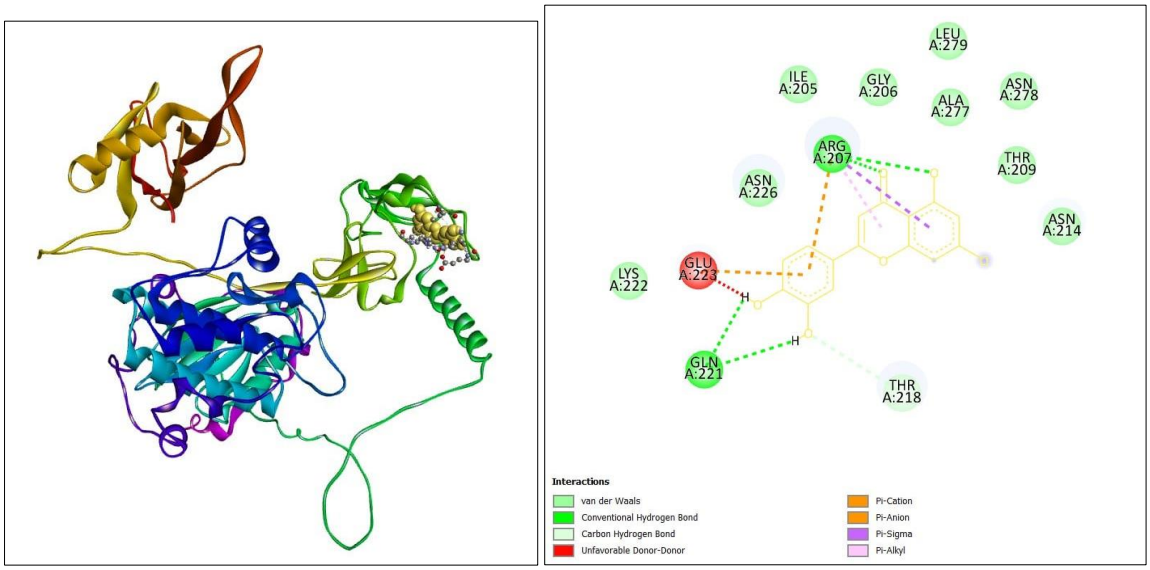
LEU A:279
ILE A:205
GLY A:206
ASN A:278
ALA A:277
ARG A:207
THR A:209
ASN A:226
ASN A:214
LYS A:222
GLU A:223
GLN A:221
THR A:218
Interactions
van der Waals
Conventional Hydrogen Bond
Carbon Hydrogen Bond
Unfavorable Donor-Donor
Pi-Cation
Pi-Anion
Pi-Sigma
Pi-Alkyl

(J)

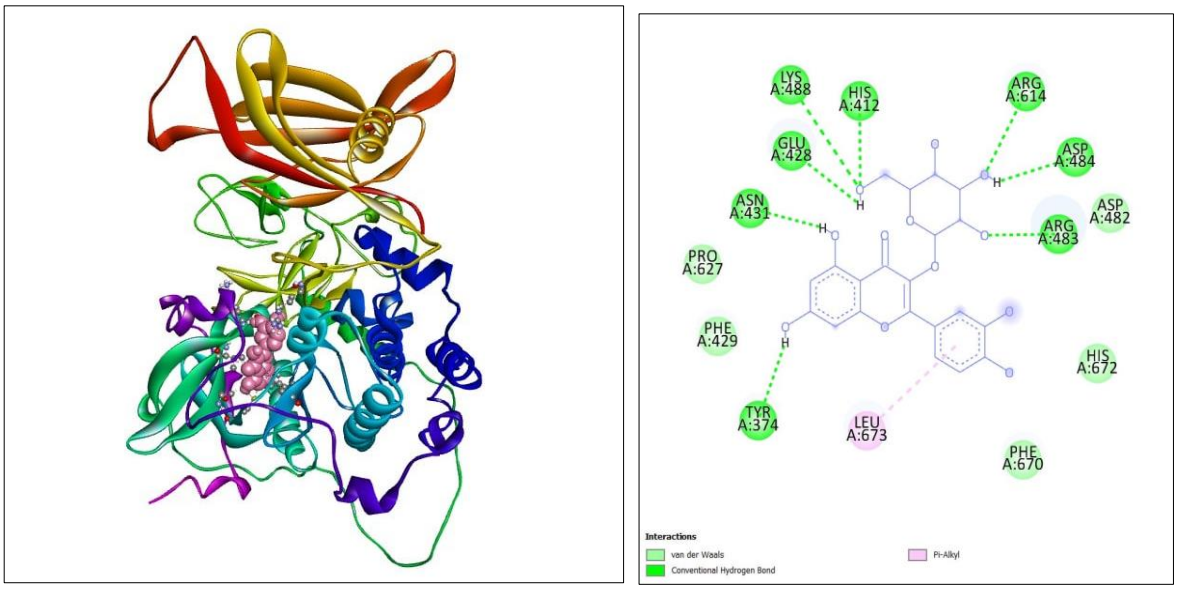
LYS A:488
HIS A:412
ARG A:614
GLU A:428
ASP A:484
ASN A:431
ASP A:482
ARG A:483
PRO A:627
PHE A:429
HIS A:672
TYR A:374
LEU A:673
PHE A:670
Interactions
van der Waals
Conventional Hydrogen Bond
Pi-Alkyl

(K)

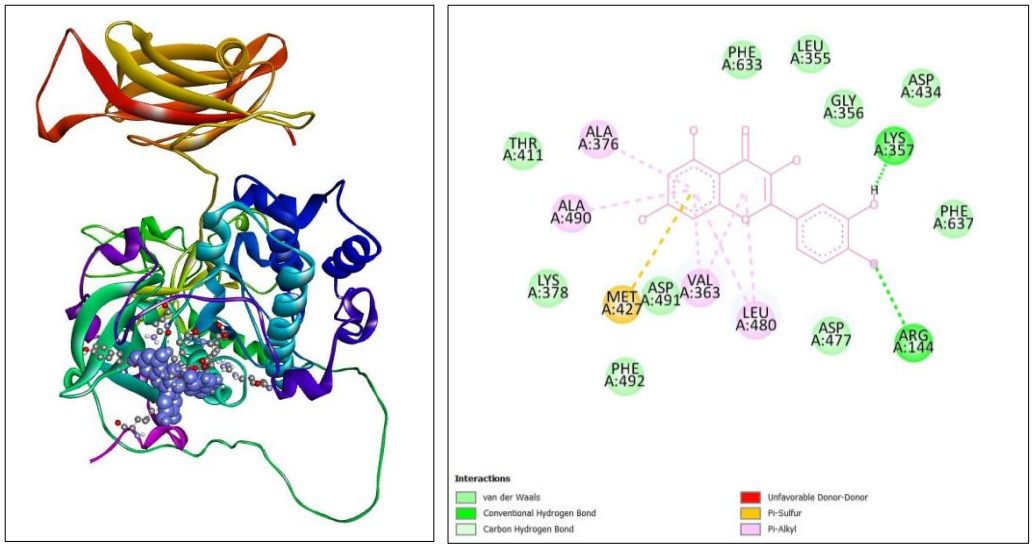
PHE A:633
LEU A:355
ASP A:434
GLY A:356
THR A:411
ALA A:376
LYS A:357
ALA A:490
PHE A:637
LYS A:378
MET A:427
ASP A:491
VAL A:363
LEU A:480
ASP A:477
ARG A:144
PHE A:492
Interactions
van der Waals
Conventional Hydrogen Bond
Carbon Hydrogen Bond
Unfavorable Donor-Donor
Pi-Sulfur
Pi-Alkyl

(L)

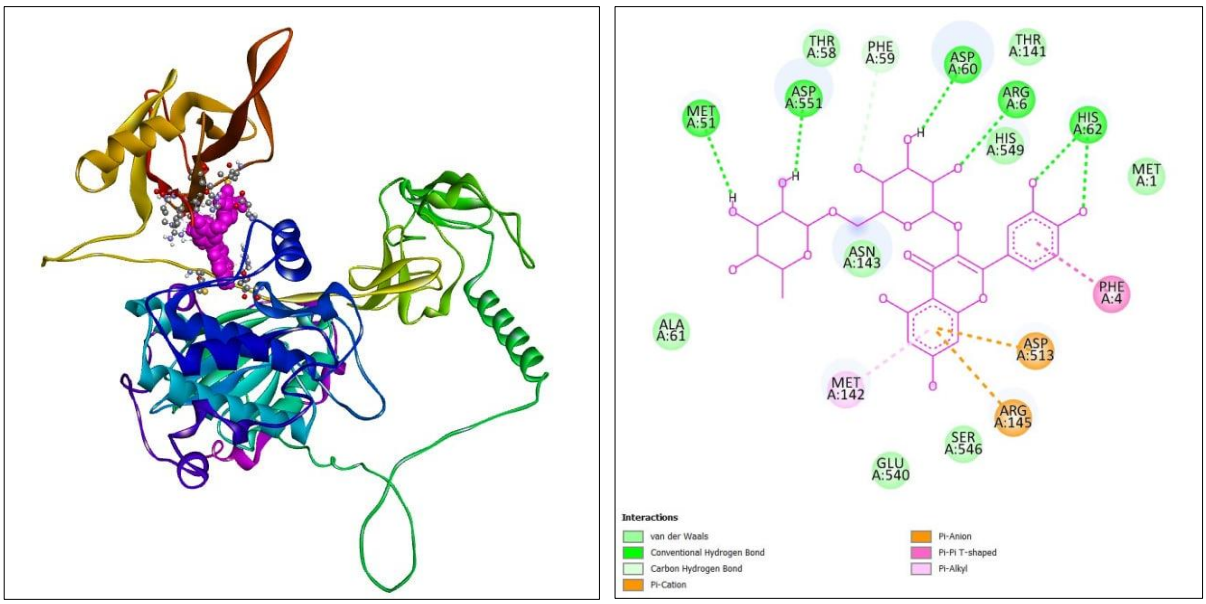
THR A:58
PHE A:59
ASP A:60
THR A:141
ASP A:551
ARG A:6
MET A:51
HIS A:62
HIS A:549
MET A:1
ASN A:143
PHE A:4
ALA A:61
ASP A:513
MET A:142
ARG A:145
SER A:546
GLU A:540
Interactions
van der Waals
Conventional Hydrogen Bond
Carbon Hydrogen Bond
Pi-Cation
Pi-Anion
Pi-Pi T-shaped
Pi-Alkyl

(M)

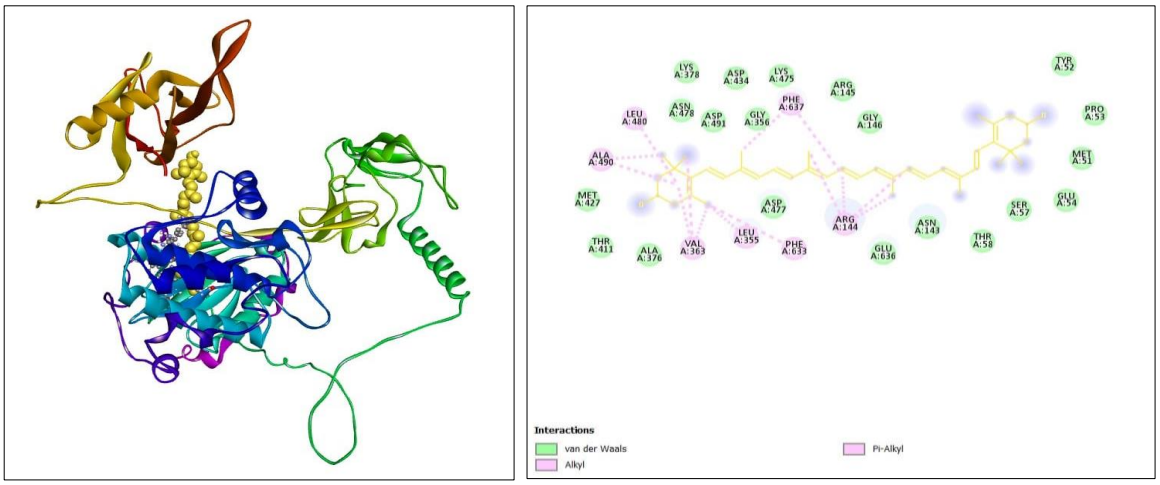

(N)

Figure 6 (a-n): 3D and 2D representation of protein ligand interaction: (a) Alpha-carotene (b) Beta-carotene (c) Caffeic acid (d) Chlorogenic acid (e) p-coumaric acid (f) Ferulic acid (g) Gallic acid (h) Kaempferol-3-glucoside (i) Lutin (j) Luteolin (k) Quercetin (l) Isoquercetin (m) Rutin (n) Zeaxanthin. Light green colour denotes Van der Waal interaction, pink colour shows pi interaction and dark green colour showcases hydrogen bonding.

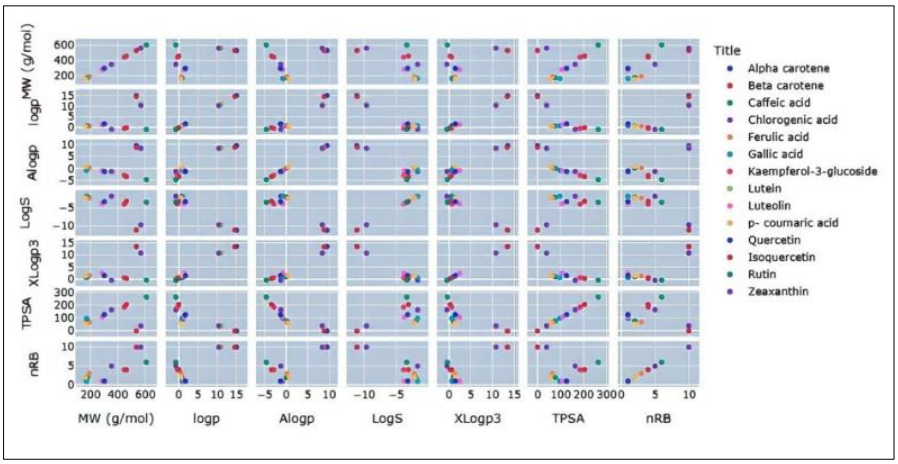

Figure 7: Comparative depiction of observed topological polar surface area (TPSA), molecular weight (MW), sp3 hybridization, logS (solubility), xlogP3 and nRB value for compounds with standard values. The standardised values are as follows; TPSA: 20-130 Å^2; logS: <6; sp3 hybridization: >0.25; MW: <500; nRB: <9; xlogP3: -0.7- +5.0

Acknowledgement

Authors would like to acknowledge Prof. Nazura Usmani's laboratory, Department of Zoology, Aligarh Muslim University, for providing facilities required for the work.

Disclosure

Ethical approval: Study does not require any kind of ethical approval as it completely relies on use of computational techniques and models.

Competing interest: Authors declares no conflict of interest.

Funding: No funding was granted for this study from any source.

ORCID ID

Mudassir Alam: https://orcid.org/0000-0001-8255-0273
Kashif Abbas: https://orcid.org/0000-0002-1337-6061
Mohd Faizan Saifi: https://orcid.org/0009-0008-2310-5602
S. Mohd. Hasan Abedi: https://orcid.org/0009-0002-6497-6283
Mohsin Hussain: https://orcid.org/0000-0001-7448-2880
Sahab Kausar: https://orcid.org/0000-0001-9543-1847

REFERENCES

1. Singh AK, Kumar R, Pandey AK. Hepatocellular Carcinoma: Causes, Mechanism of Progression and Biomarkers. Curr Chem Genom Transl Med. 2018;12:9-26.
2. Kneeman JM, Misdraji J, Corey KE. Secondary causes of nonalcoholic fatty liver disease. Therap Adv Gastroenterol. 2012;5(3):199-207.
3. He S, Li Q, Huang Q, Cheng J. Targeting protein kinase C for cancer therapy. Cancers. 2022;14(5):1104.
4. Black AR, Black JD. Protein kinase C signaling and cell cycle regulation. Front Immunol. 2013;3:423.
5. Kolczynska K, Loza-Valdes A, Hawro I, Sumara G. Diacylglycerol-evoked activation of PKC and PKD isoforms in regulation of glucose and lipid metabolism: a review. Lipids Health Dis. 2020;19(1):113.
6. Newton AC, Bootman MD, Scott JD. Second Messengers. Cold Spring Harb Perspect Biol. 2016;8(8):a005926.
7. Oikawa T, Yamada K, Tsubota A, et al. Protein kinase C Delta is a novel biomarker for hepatocellular carcinoma. Gastro Hep Advances. 2023;2(1):83-95. doi:10.1016/j.gastha.2022.07.020
8. Mármol I, Sánchez-De-Diego C, Jiménez-Moreno N, Ancín-Azpilicueta C, Rodríguez-Yoldi MJ. Therapeutic Applications of

Rose Hips from Different Rosa Species. International Journal of Molecular Sciences. 2017;18(6):1137.
9. Medveckienė B, Kulaitienė J, Jarienė E, Vaitkevičienė N, Hallman E. Carotenoids, Polyphenols, and Ascorbic Acid in Organic Rosehips (Rosa spp.) Cultivated in Lithuania. Applied Sciences. 2020;10(15):5337.
10. Zhou L. Serum tumor markers for detection of hepatocellular carcinoma. World Journal of Gastroenterology. 2006;12(8):1175
11. Ren Z, Ma X, Duan Z, Chen X. Diagnosis, therapy, and prognosis for hepatocellular carcinoma.
12. Analytical Cellular Pathology. 2020;2020:1-2.
13. UniProt: the universal protein knowledgebase. Nucleic Acids Research. 2016;45(D1):D158-D169
14. Waterhouse A, Bertoni M, Bienert S, et al. SWISS-MODEL: homology modelling of protein structures and complexes. Nucleic Acids Research. 2018;46(W1):W296-W303.
15. Laskowski RA, MacArthur MW, Moss DS, Thornton JM. PROCHECK: a program to check the stereochemical quality of protein structures. Journal of Applied Crystallography. 1993;26(2):283-291.
16. Chen VB, Arendall WB, Headd JJ, et al. MolProbity: all-atom structure validation for macromolecular crystallography. Acta Crystallographica Section D: Structural Biology. 2009;66(1):12-21.
17. O'Boyle NM, Banck M, James CA, Morley C, Vandermeersch T, Hutchison G. Open Babel: An open chemical toolbox. Journal of Cheminformatics. 2011;3(1).
18. Dallakyan S, Olson AJ. Small-Molecule Library Screening by Docking with PyRx. In: Methods in Molecular Biology. ; 2014:243-250.
19. Trott O, Olson AJ. AutoDock Vina: Improving the speed and accuracy of docking with a new scoring function, efficient optimization, and multithreading. Journal of Computational Chemistry. 2009;31(2):455-461.
20. Discovery Studio Modeling Environment, Release 4.5. 2021. BIOVIA, Dassault Systèmes, San Diego.
21. Brenk R, Schipani A, James DB, et al. Lessons Learnt from Assembling Screening Libraries for Drug Discovery for Neglected Diseases. ChemMedChem. 2008;3(3):435-444.
22. Lipinski CA, Lombardo F, Dominy BW, Feeney PJ. Experimental and computational approaches to estimate solubility and permeability in drug discovery and development settings 1PII of original article: S0169-409X(96)00423-1. The article was originally published in Advanced Drug Delivery Reviews 23 (1997) 3–25. 1. Advanced Drug Delivery Reviews. 2001;46(1-3):3-26.
23. Daina A, Michielin O, Zoete V. SwissADME: a free web tool to evaluate pharmacokinetics, drug-likeness and medicinal chemistry friendliness of small molecules. Scientific Reports. 2017;7(1).
24. Cheng F, Li W, Zhou Y, et al. AdMetSAR: a comprehensive source and free tool for assessment of chemical ADMET properties. Journal of Chemical Information and Modeling. 2012;52(11):3099-3105.
25. Banerjee P, Eckert A, Schrey AK, Preißner R. ProTox-II: a webserver for the prediction of toxicity of chemicals. Nucleic Acids Research. 2018;46(W1):W257-W263.
26. Filimonov DA, Lagunin AA, Gloriozova TA, Rudik AV, Druzhilovskii DS, Pogodin PV, et al. Prediction of the Biological Activity Spectra of Organic Compounds Using the Pass Online Web Resource. Chemistry of Heterocyclic Compounds. 2014;50(3):444-57.
27. Sun Y, Zhou M, Luo L, Pan H, Zhang Q, Yu C. Metabolic profiles, bioactive compounds and antioxidant activity of rosehips from xinjiang, China. LWT. 2023 Jan 15;174:114451.
28. Tumbas VT, Canadanović-Brunet JM, Cetojević-Simin DD, Cetković GS, Ethilas SM, Gille L. Effect of rosehip (Rosa canina L.) phytochemicals on stable free radicals and human cancer cells. J Sci Food Agric. 2012;92(6):1273-1281.

HOW TO CITE THIS ARTICLE
Alam M, Abbas K, Saifi MF, Abedi SMH, Hussain M, Kausar S. Rosehip Phytochemicals: A Computational Approach for Inhibiting Protein Kinase C Delta in Hepatocellular Carcinoma Treatment. J Phytopharmacol 2023; 12(6):341-357. doi: 10.31254/phyto.2023.12601